IEEE Access
Multidisciplinary | Rapid Review | Open Access Journal

Received 14 May 2023, accepted 13 June 2023, date of publication 23 June 2023, date of current version 18 July 2023.

Digital Object Identifier 10.1109/ACCESS.2023.3288833

RESEARCH ARTICLE

Analysis of Selective User Forwarding in Cell-Free Massive MIMO With Channel Aging

MARIA FRANCIS[1], (Student Member, IEEE), FARHAD MEHRAN[2], (Senior Member, IEEE), AND K. V. S. HARI[1]

[1]Department of Electrical Communication Engineering, Indian Institute of Science, Bengaluru 560012, India
[2]BT (British Telecom) labs, IP5 3RE Adastral Park, U.K.

Corresponding author: Maria Francis (mariafrancis@iisc.ac.in)

This work was supported by the British Telecom India Research Centre (BTIRC).

ABSTRACT Cell-free massive multiple-input-multiple-output (CF-mMIMO) systems provide spectral efficiency (SE) gains with a more uniform quality-of-service in the network area compared to cellular massive MIMO schemes but at the expense of higher capacity requirements on the fronthaul links. To reduce the signaling overhead on fronthaul links, we propose a selective user forwarding method for uplink data transmissions in CF-mMIMO systems, where each access point (AP) forwards the data of only a selected subset of users to the central processing unit (CPU) for joint processing. The simulation results show that the selective user forwarding scheme achieves nearly the same performance as a CF-mMIMO system with selected number of users, M, being equal to less than one-fourth of the total number of users in the network and resulting in a fronthaul signaling savings of about 75%. We then analytically study the performance of the proposed system in the presence of channel aging by deriving expressions for SE. The numerical evaluation of these expressions is shown to be close to the simulation results.

INDEX TERMS Cell-free massive MIMO (CF-mMIMO), central processing unit (CPU), channel state information (CSI), channel aging, minimum mean square error (MMSE).

I. INTRODUCTION

In cell-free massive MIMO (CF-mMIMO) systems [1], [2], [3], a large number of geographically distributed access points (APs) jointly serve a relatively small number of users by spatially multiplexing them on the same time-frequency resources [4]. The coherent transmission in the downlink and coherent reception in the uplink are coordinated by the central processing unit (CPU). The APs are connected to the CPU through wired/wireless fronthaul links. The coherent processing allows CF-mMIMO to achieve more than ten times improvement in the 95%-likely spectral efficiency (SE) compared to small-cell networks, where the APs serve a set of UEs within the cell and there is no cooperation among the APs [4]. The performance of CF-mMIMO has been studied for different channel models such as spatially correlated Rayleigh fading channels in [2] and [5] and with Rician faded channels in [6].

The associate editor coordinating the review of this manuscript and approving it for publication was Bilal Khawaja.

One of the major challenges in the practical implementation of CF-mMIMO is the huge signaling overhead it adds to the fronthaul links. This is due to the fact that all the UEs are coherently served by all the APs in the system [4]. This requires the CPU to send the downlink data to all the APs and receive the uplink data from all the APs. The high amount of data that needs to be transmitted between the CPU and the APs results in a substantial increase in signaling over the fronthaul links. This is in contrast to the conventional massive MIMO, which requires only one or a few high-capacity links that connect the AP (equipped with a large number of antennas) to the core network. Hence the fronthaul links need to be carefully designed to ensure that they can support the bandwidth requirements of CF-mMIMO.

Also to realize the SE gains of CF-mMIMO, accurate channel state information (CSI) is required at the CPU for transmit beamforming in the downlink and receive combining in the uplink. Due to the limitations in acquiring downlink CSI, the time-division-duplex (TDD) mode of operation is commonly employed for CF-mMIMO systems [4]. It allows

the CPU to infer the downlink CSI from uplink pilot symbols by exploiting channel reciprocity. Although the pilot symbols are transmitted at every coherence block, in some cases (e.g., mobility scenarios) the estimated CSI can be outdated with respect to the actual channel conditions during the data transmission phase. This is because the channel gains vary continuously over time when there is a relative motion between the transmitter and receiver. Thus, at the CPU, the downlink beamforming and uplink combining vectors will be calculated based on outdated CSI, which may not be optimal for the channel gains at the time of data transmission. This leads to a loss in SE, which is referred to as Doppler-induced channel aging [7], [8].

In this work, we propose a selective user forwarding for CF-mMIMO, in which each AP forwards the data of only a fixed number of UEs to the CPU. This significantly reduces the fronthaul signaling. Also, we analytically evaluate the impact of channel aging on CF-mMIMO systems with selective user forwarding in the uplink.

A. RELATED LITERATURE

In this section, we review the prior works on reducing the fronthaul overhead, channel aging, and performance analysis in CF-mMIMO.

1) FRONTHAUL OVERHEAD REDUCTION

CF-mMIMO network assumes that all the APs are connected to a central entity/CPU, which is responsible for coordinating and processing the signals of all the UEs. This, in turn, results in higher computational complexity and the signaling overhead on fronthaul link (which will increase linearly with system dimensions). To relax these complexities, an architecture in which only a subset of APs serve a particular UE in the system is proposed. Different AP clustering schemes (to select the set of APs to serve a particular UE) are proposed in [3], [9], [10], [11], [12], [13], [14], [15], [16], [17], [18], and [19]. The cluster formation can be user-centric [3], [9], [10], [11], [12], [13], [14], [15] or network-centric [16], [17], [18], [19]. In the user-centric architecture, each user is served by a subset of APs which are close to it. Generally, the serving APs are selected based on channel conditions as in [10], [13], and [14]. In [3], a scalable CF-mMIMO is proposed based on the concept of dynamic cooperation clustering (DCC), which has originated from network MIMO literature. DCC provides an algorithm for joint initial access, pilot assignment, and cluster formation. In network-centric architecture, UEs are grouped into disjoint set of clusters, and each UE set is served by a cluster of APs.

2) CHANNEL AGING

Due to the time-varying nature of the wireless channel, the CSI used for computing beam-forming/combining vectors might be different from the actual CSI at the time of data transmission/reception. The authors of [7] use channel prediction to compensate the effects of channel aging in massive MIMO downlink/uplink, and it has been shown that this approach allows to overcome the detrimental effects of channel aging partially. Furthermore in [8], [20], [21], and [22], the effects of channel aging with different precoding/combining schemes taking into consideration different practical aspects such as phase noise and hardware impairments is discussed. In [23] an FDD conventional massive MIMO is considered, and the effect of channel aging is studied for both uplink and the downlink by deriving the deterministic equivalents for the achievable rates. The authors of [24] consider the FDD massive MIMO performance in downlink, with predicted channel gains to combat channel aging. Channel aging is shown to significantly degrade the performance in a line of sight (LOS) environment [25] for a multi-user MIMO.

The authors of papers [26], [27], [28] obtain expression to study the performance of CF-mMIMO systems under channel aging conditions. In [26], the downlink performance of CF-mMIMO systems with zero-forcing precoding is considered and authors also consider the effect of phase noise in the analysis. In [27], authors derive a lower bound for the achievable rate in the presence of channel aging and show that the CF-mMIMO systems perform better than small cells for uplink under mobility scenarios. The authors of [28] derive a deterministic equivalent for instantaneous SINR, using fixed point iteration for the uplink of CF-mMIMO under channel aging scenario.

B. CONTRIBUTIONS

We propose an AP-centric *selective user forwarding* approach for the uplink in a CF-mMIMO system to reduce the fronthaul signaling overhead. Here, each AP independently selects a few users based on certain criteria and serves only those users. In this case, as each AP sends/receives data to/from the users it serves, fronthaul signaling will be significantly reduced. As will be shown later on (Section VI), this might lead to a negligible or small loss in SE performance as a user is now served by a subset of APs and not all the APs.

The feature of the proposed approach that distinguishes it from the user-centric approach is that the selective user forwarding scheme is where the AP is selecting a set of best M UEs. This architecture provides a key advantage of carrying out the deterministic design of the fronthaul traffic avoiding worst-case designs. In user-centric networks, the fronthaul capacity dimensioning is user-traffic dependent and must be done for the worst-case traffic, because the number of UEs served by a particular AP would be variable. To support that, the fronthaul should be designed to accomodate the worst-case traffic. Also, in the proposed scheme, the UE selection is based on the long-term channel statistics which remain constant for several coherence intervals, so the APs select the users once in a few coherence time intervals. In the user-centric approach [14], [15], the selection is based on instantaneous channel gains and UEs selection is done once in every coherence interval.

Also, to study the performance of the proposed system under channel aging, we derive tractable expressions which depend only on the spatial covariance matrices for minimum mean squared error (MMSE) based combining in the uplink. This allows us to analytically study the performance of the system with channel aging even when the number of APs and the number of UEs are very high for which the time and computational effort involved in the system-level Monte Carlo simulations is very high. The main contributions of the paper can be summarized as follows.

- We propose an AP-centric scheme to reduce the fronthaul overhead of CF-mMIMO. In the proposed scheme only a fixed number of UEs are served by each AP. This also enables the deterministic design of the fronthaul traffic, in addition to significantly reducing the fronthaul signaling.
- We study the performance degradation of the proposed system for MMSE combining under channel aging and compare it with the case when CPU has perfect CSI. This allows us to quantify the degradation in SE that results from using a combining vector optimized for perfect CSI (the MMSE combining vector) when only aged/outdated CSI is available.
- We derive novel tractable expressions to approximate SE only in terms of the long-term statistics of the channel, both for the cases of perfect CSI and outdated CSI is available at the CPU. The derived expressions are devoid of any iterative terms as in [28] and hence do not require any convergence guarantees.
- The derived expressions are asymptotic and we show that they are quite accurate in predicting the system behavior even for system dimensions in the range of what we have in practical scenarios.

C. ORGANIZATION & NOTATIONS

The remainder of the paper is organized as follows. Section II describes the system model. The uplink CF-mMIMO processing is described in section III and selective user forwarding for CF-mMIMO is detailed in section IV. The performance analysis for perfect and outdated CSI scenarios is shown in section V. Section VI presents the simulation results followed by conclusions in section VII.

We denote vectors and matrices by bold-faced lower case and upper case letters, respectively. The $n \times n$ identity matrix is represented by $\boldsymbol{I}_n$. We use superscripts, $(.)^*$, $(.)^T$ and $(.)^H$ to represent conjugate, transpose and conjugate transpose respectively. We denote a diagonal matrix as, $\text{diag}(x_1, \ldots x_n)$, with $x_1, \ldots, x_n$ as the diagonal elements. We denote the absolute value, expectation, and trace operator as $|\cdot|$, $\mathbb{E}(\cdot)$, and $\text{tr}(\cdot)$, respectively. Finally, $\boldsymbol{x} \sim \mathcal{CN}(\boldsymbol{0}, \boldsymbol{R})$ denotes a circularly symmetric complex Gaussian random vector $\boldsymbol{x}$ with zero mean vector and covariance matrix $\boldsymbol{R}$. The cardinality of set $\mathcal{S}$ is denoted as $|\mathcal{S}|$. The frequently used symbols are cataloged in Table 1.

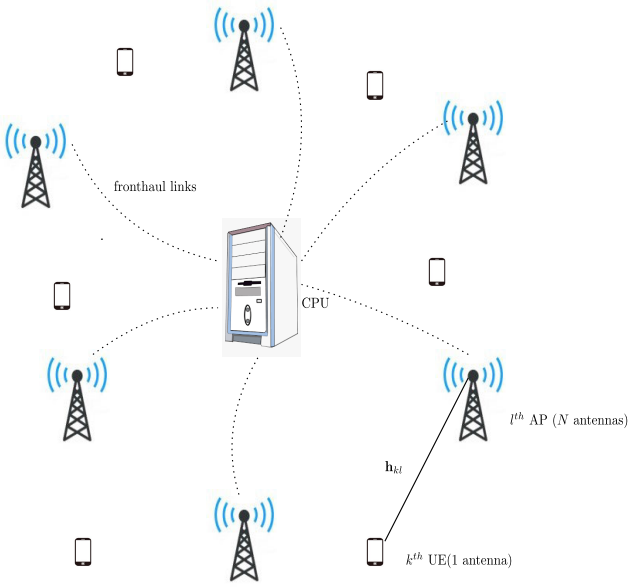

FIGURE 1. A CF-mMIMO system with K UEs coherently served by L APs in the network. All the activities of APs are coordinated by a CPU, and APs to the CPU are connected through fronthaul links. Each UE has 1 antenna and each AP has N antennas.

II. SYSTEM MODEL

We consider the uplink of a CF-mMIMO system with L APs, each equipped with N antennas that serve K single antenna users as illustrated in Fig. 1. The APs to CPU are connected through fronthaul links. In this work, our focus will be on the uplink scenario as many services such as machine-type communications, Internet of Things (IoT), etc., are uplink-centric.

A. CHANNEL MODEL

We model the channel gain between k^{th} UE and l^{th} AP at n^{th} symbol time, $\boldsymbol{h}_{kl}[n]$, as Rayleigh distributed, i.e., $\boldsymbol{h}_{kl}[n] \sim \mathcal{CN}(0, \boldsymbol{R}_{kl})$. It is assumed to be independent across all APs and UEs. The complex normal Gaussian distribution models the small-scale fading and, $\boldsymbol{R}_{kl}$, models the large-scale fading characteristics of the channel such as path loss, shadowing, antenna gains, and spatial correlation [29].

The $(u, v)^{th}$ element of $\boldsymbol{R}_{kl}$ is given by [29, Section 2.6],

$$[\boldsymbol{R}_{kl}]_{u,v} = \beta_{kl} e^{2\pi d_{\text{H}}(u-v)\sin\varphi} e^{-\frac{\sigma_\varphi^2}{2}(2\pi d_{\text{H}}(u-v)\cos\varphi)^2}, \quad (1)$$

where φ is the nominal angle of arrival of the rays to the AP antennas, d_H is the height of the AP from the ground level. The standard deviation, ($\sigma_\varphi \geq 0$) is the angular standard deviation and determines how large the deviations from the nominal angle are. The eigen-structure of $\boldsymbol{R}_{kl}$ determines the spatial channel correlation of the channel $\boldsymbol{h}_{kl}$, *i.e.*, which spatial directions are likely to contain strong signal components than other directions. Strong spatial correlation is characterized by large eigen-value variations.

TABLE 1. List of Symbols.

Symbol	Definition	Symbol	Definition
L	Number of APs	K	Number of UEs
N	Number of antennas connected to each AP	M	Number of UEs forwarded by each AP.
$\boldsymbol{h}_{kl}[n]$	Channel gain vector between k^{th} UE and l^{th} AP at n^{th} time instant.	$\boldsymbol{R}_{kl}$	Spatial covariance matrix between k^{th} UE and l^{th} AP.
β_{kl}	Large-scale fading coefficients between k^{th} UE and l^{th} AP.	d_{kl}	De-correlation distance between k^{th} UE and l^{th} AP.
d_H	Height of the AP from the ground.	F_{kl}	Log-normal shadow fading between k^{th} UE and l^{th} AP.
v_k	Combining vector in the uplink for the k^{th} user at the CPU.	p_k	Uplink transmitting power of the k^{th} user.
$\boldsymbol{h}_{k\mathcal{L}_k}$	Channel gain vector between k^{th} UE and $\mathcal{L}_k$ APs.	$\boldsymbol{v}_k^{\text{sf}}$	Combining vector for k^{th} user in selective user forwarding.
ρ	Temporal correlation coefficient.	$\boldsymbol{w}_{kl}[n]$	Independent innovation component at the n^{th} time instant.
T_s	Symbol duration.	d	Delay in symbol times.
$\mathscr{L}_k$	Set of APs that reported k^{th} UE as one of its best user	$\mathscr{M}_l$	Set of M UEs reported by the l^{th} AP.
T_k	Cardinality of $\mathscr{L}_k$	N_t	Number of observations which are averaged out for β_{kl} values.

The large-scale fading coefficients between k^{th} user and l^{th} AP, β_{kl}, is modelled using the 3GPP Urban Microcell model as [30, Table B.1.2.2],

$$\beta_{kl}[\text{dB}] = -30.5 - 36.7\log_{10}\left(\frac{d_{kl}}{1\text{ m}}\right) + F_{kl}, \qquad (2)$$

where d_{kl} denotes the minimum distance between k^{th} UE and l^{th} AP across all wrap-around cases (to provide a uniform scattering environment), and $F_{kl} \sim \mathcal{N}\left(0, 4^2\right)$ models the log-normal shadow fading. The correlation between shadow fading coefficients is modelled as [30, Table B.1.2.1],

$$\mathbb{E}\left\{F_{kl}F_{ij}\right\} = \begin{cases} 4^2 \;\; 2^{-\delta_{ki}/9\text{m}} & l = j \\ 0 & l \neq j \end{cases} \qquad (3)$$

where δ_{ki} is the distance between UE k and UE i.

Note that, $\sum_{n=1}^{N_t} \frac{1}{N_t}|\boldsymbol{h}_{kl}[n]|^2 \xrightarrow[N_t\to\infty]{a.s} \mathbb{E}\{\|\boldsymbol{h}_{kl}\|^2\}$, from the law of large numbers and hence we have $\beta_{kl} = \text{tr}(\boldsymbol{R}_{kl})/N$.

B. CHANNEL AGING MODEL

Under the channel aging scenario, the channel gains $\boldsymbol{h}_{kl}[n]$ vary as a function of symbol index time, n, causing the channel gains to be correlated across time. Hence, the channel gains, $\boldsymbol{h}_{kl}[n]$ varies as a function of n and is correlated with the delayed channel gains $\boldsymbol{h}_{kl}[n-d]$. Here d denotes the aging parameter, in terms of number of delayed symbols. Since these are jointly distributed Gaussian random vectors, their joint distribution is completely specified by $\boldsymbol{R}_{kl}$ and the temporal correlation coefficient ρ. For Jake's fading model, $\rho = J_0(2\pi f_d d T_s)$, where $J_0(\cdot)$ is the modified Bessel function of the first kind and order zero, f_d is the maximum Doppler shift, and T_s is the symbol duration. We consider the following model in this paper,

$$\boldsymbol{h}_{kl}[n] = \rho\boldsymbol{h}_{kl}[n-d] + \sqrt{1-|\rho|^2}\boldsymbol{w}_{kl}[n], \qquad (4)$$

where $\boldsymbol{w}_{kl}[n]$ is the independent innovation component that has the same distribution as of the channel vector $\boldsymbol{h}_{kl}[n]$.

III. UPLINK CELL-FREE MASSIVE MIMO PROCESSING

The uplink processing of the CF-mMMO generally consists of the training phase and the data transmission phase. In the training phase, the UEs transmit uplink pilot symbols, from which the CPU obtains the CSI. In this work, we assume that CPU has access to perfect CSI without any estimation errors. The training phase is followed by the data transmission phase, where each UE sends uplink data symbols. The different steps involved in the CF-mMIMO processing are summarized in Table 2.

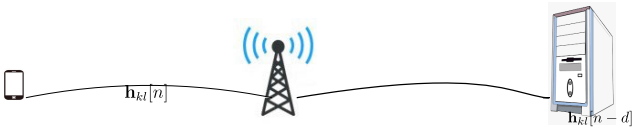

FIGURE 2. Illustration of channel aging where there is a delay of d symbol times for processing the data at the CPU transmitted at n^{th} time instant.

A. UPLINK RECEIVE COMBINING

In this step, the CPU computes the combining vector to detect the data transmitted by each user. For the perfect CSI scenario, the CPU computes the MMSE combining vector, $\boldsymbol{v}_k^{\text{per}}[n]$, for the user, k, based on the channel gains at time instant n, and is given by

$$\boldsymbol{v}_k^{\text{per}}[n] = p_k\left[\sum_{i=1}^{K} p_i\boldsymbol{h}_i[n]\boldsymbol{h}_i^H[n] + \sigma^2\boldsymbol{I}\right]^{-1}\boldsymbol{h}_k[n]. \qquad (5)$$

Here, $\boldsymbol{h}_i[n] = [\boldsymbol{h}_{i1}^T[n], \ldots, \boldsymbol{h}_{iL}^T[n]]^T$ is the LN-length vector of channel gains to all the APs from user i at time n and p_k is the uplink transmit power of the k^{th} UE. Note that the MMSE combining vectors at time n are computed based on channel gains at symbol time n, and are optimal in the sense that they maximize the SINRs of users [29].

In the channel aging case, the CPU uses the combining vector $\boldsymbol{v}_k[n]$ at symbol time n, computed from channel gains $\boldsymbol{h}_{kl}[n-d]$ at symbol time $n-d$, for signal combining at the receiver. Here, delay d models the outdated nature of CSI at CPU (due to the time difference between the time at which the channel is measured and is used for processing), fronthaul propagation delay (due to the finite capacity of fronthaul), and CPU processing delays. A pictorial representation of the channel aging scenario is shown in Fig. 2. The channel gains at CPU are delayed by d symbol times. In that event, the MMSE combining vector is calculated as a function of

TABLE 2. Summary of the steps involved in the uplink processing of the data send by a k^{th} user in CF-mMIMO and CF-mMIMO with SUF.

		Conventional CF-mMIMO	CF-mMIMO with selective user forwarding (SUF CF-mMIMO)
Uplink pilot transmission phase	AP	Estimates $\boldsymbol{h}_{kl} \in \mathscr{C}^{N\times 1}$ from uplink pilots received from UEs $k \in \{1,\ldots,K\}$.	Estimates $\boldsymbol{h}_{kl} \in \mathscr{C}^{N\times 1}$ from uplink pilots received from UEs $k \in \{1,\ldots,K\}$.
			Estimate $\hat{\beta}_{kl}$, as $\hat{\beta}_{kl} = \frac{1}{NN_t}\sum_{n=1}^{N_t} \boldsymbol{h}_{kl}^{\mathrm{H}}[n]\boldsymbol{h}_{kl}[n]$.
			Sort $\hat{\beta}_{kl}$in descending order and selects best-M user set as $\mathscr{M}_l = k_{1,l},\ldots,k_{l,M}$.
			Send the indices of the best-M UEs to the CPU.
	CPU	Computes MMSE combining vector, $\boldsymbol{v}_k^{\mathrm{per}}$ using equation (5).	Computes MMSE combining vector, $\boldsymbol{v}_k^{\mathrm{sf}}$ using equation (10) and substituting $d = 0$.
		Sends $\boldsymbol{v}_{kl} \in \mathscr{C}^{N\times 1}$ to the l^{th} AP for $l \in \{1,\ldots,L\}$.	Sends $\boldsymbol{v}_{kl}^{\mathrm{sf}} \in \mathscr{C}^{N\times 1}$ to l^{th} AP for $l \in \mathscr{L}_k$.
Uplink data transmission phase	AP	AP makes local estimate $\tilde{s}_{kl} = \boldsymbol{v}_{kl}^{\mathrm{H}}\boldsymbol{y}_l$.	AP makes local estimate, $\tilde{s}_{kl} = (\boldsymbol{v}_{kl}^{\mathrm{sf}})^H\boldsymbol{y}_l$.
		Sends the local estimate to the CPU.	Sends the local estimate to the CPU.
	CPU	CPU combines $\tilde{s}_{kl}$ from all APs as $\hat{s}_k = \sum_{l=1}^{L}\tilde{s}_{kl}$.	CPU combines $\tilde{s}_{kl}$ from APs in $\mathscr{L}_k$ as $\hat{s}_k = \sum_{l\in\mathscr{L}_k}\tilde{s}_{kl}$.

outdated CSI, $\boldsymbol{h}_i[n-d]$, and for $i = 1,\ldots,K$. It is given by,

$$\boldsymbol{v}_k[n] = p_k\left[\sum_{i=1}^{K} p_i\boldsymbol{h}_i[n-d]\boldsymbol{h}_i^H[n-d] + \sigma^2\boldsymbol{I}\right]^{-1}\boldsymbol{h}_k[n-d]. \tag{6}$$

Note that, $\boldsymbol{v}_k^{\mathrm{per}}[n]$ is a special case of $\boldsymbol{v}_k[n]$ when $d = 0$. Here, the CPU is unaware of the outdated nature of CSI and computes as if they are perfect.

B. UPLINK DATA TRANSMISSION

The CPU uses the combining vector $\boldsymbol{v}_k[n]$ to detect the symbol s_k sent by user k at time n from the received symbol vector $\boldsymbol{y}_k[n] = [\boldsymbol{y}_1^T[n],\ldots,\boldsymbol{y}_L^T[n]]^T$, for $k = 1,\ldots,K$. Here, $\boldsymbol{y}_l^T[n]$ is the symbol vector received by AP l at time n, and is expressed as

$$\boldsymbol{y}_l[n] = \sum_{i=1}^{K}\boldsymbol{h}_{il}[n]s_i[n] + \boldsymbol{n}_l[n], \tag{7}$$

where $\boldsymbol{n}_l[n]$ is the additive white Gaussian noise (AWGN) at the l^{th} AP. An estimate $\hat{s}_k[n]$ of the symbol $s_k[n]$ is computed by the CPU as $\hat{s}_k[n] = \boldsymbol{v}_k^{\mathrm{H}}[n]\boldsymbol{y}_k[n]$. Hence, the average SE of user k is given by [29]

$$\mathrm{SE}_k[n] = \mathbb{E}\log_2(1 + \mathrm{SINR}_k[n]), \tag{8}$$

where, $\mathrm{SINR}_k[n]$ is the instantaneous signal-to-interference-ratio of the k^{th} user at the n^{th} time instant, and is given by,

$$\mathrm{SINR}_k[n] = \frac{p_k|\boldsymbol{v}_k^{\mathrm{H}}[n]\boldsymbol{h}_k[n]|^2}{\sum_{i=1,i\neq k}^{K} p_i|\boldsymbol{v}_k^{\mathrm{H}}[n]\boldsymbol{h}_i[n]|^2 + \sigma^2\|\boldsymbol{v}_k[n]\|^2}. \tag{9}$$

Note that the delayed nature of the channel is embodied in the combining vector used in the uplink.

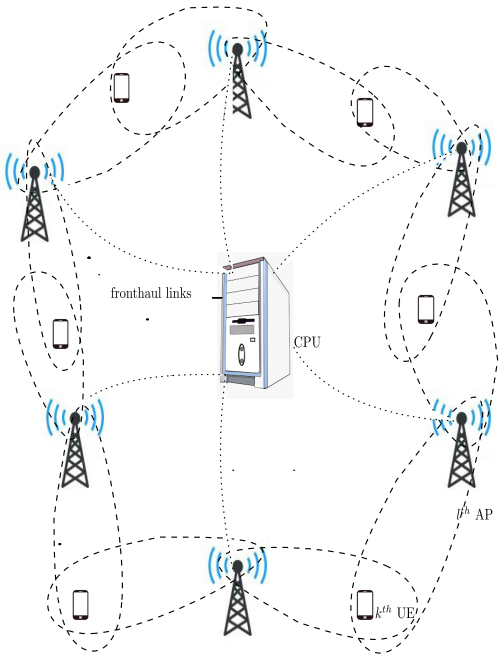

FIGURE 3. Illustration of selective user forwarding (SUF), where each AP forwards the data of 2 ($M = 2$) UEs to CPU.

IV. SELECTIVE USER FORWARDING (SUF) IN UPLINK OF CELL-FREE MASSIVE MIMO

In this section, we propose selective user forwarding to reduce the fronthaul signaling in a conventional CF-mMIMO system. In selective user forwarding, each AP serves only a subset of $M \leq K$ users and the selection of UEs is based on β_{kl} values. The algorithm to select the UEs is given in Algorithm 1. Here, the combining vector coefficients for a user are shared only with the APs that serve the user. Also,

only the serving APs forward the local symbol estimates of a user to the CPU. This helps to reduce the fronthaul signaling. The idea of selective user forwarding is illustrated in Fig. 3.

Algorithm 1 Algorithm for Selecting the Best-M Set in SUF

$M \geq 0$; & $M \leq K$

for $l = 1 : L$

1) Each AP estimates $\boldsymbol{R}_{kl}$ by time averaging the received signal over N_t coherence intervals, distributed over time and frequency, as,

$$\hat{\boldsymbol{R}}_{kl}^{\text{sample}} = \frac{1}{N_t} \sum_{n=1}^{N_t} \boldsymbol{h}_{kl}[n](\boldsymbol{h}_{kl}[n])^{\text{H}}.$$

As the number of observations, N_t becomes large, the elements of $\hat{\boldsymbol{R}}_{kl}^{\text{sample}}$ converges to true value of $\boldsymbol{R}_{kl}$.

2) Find large-scale fading coefficients β_{kl}.

$$\hat{\beta}_{kl} = \frac{1}{N} \text{tr}(\hat{\boldsymbol{R}}_{kl}^{\text{sample}})$$

3) Sort $\hat{\beta}_{kl}$ for $k \in \{1 \dots K\}$, in descending order.
4) Select the set of M users corresponding to the first M values.

end

For this process, the fronthaul signaling involved can be calculated as follows, each AP sends the estimated channel gains of all the users and the indices of best-M users to the CPU. The CPU returns with the combining vectors of M users. This happens only once in every coherence interval and involves sending $KLN + MLN + ML$ complex symbols over the fronthaul. Further, the APs compute the local estimates of the information symbols during uplink data transmission, which are forwarded to the CPU. This involves sending ML complex symbols over the fronthaul every symbol time. For CF-mMIMO, the corresponding signaling is $KLN + KLN$ complex symbols every coherence interval and KL complex symbols every symbol time. Thus, the fronthaul signaling is significantly lower when M is small. However, for small M, SE reduces as a user symbol is processed only by a smaller subset of APs.

The SINR of user k at time n, for CF-mMIMO with selective user forwarding and MMSE combining, denoted by, $\text{SINR}_k^{\text{sf}}[n]$, is calculated as follows. Let $\mathcal{L}_k$ denote the set of APs that serve user k, and T_k denotes the cardinality of the set $\mathcal{L}_k$. Then, $\hat{s}_k = \sum_{l \in \mathcal{L}_k} \left(\boldsymbol{v}_{kl}^{\text{sf}}[n]\right)^H \boldsymbol{y}_l[n]$, where $\boldsymbol{v}_{kl}^{\text{sf}}[n]$ is the vector of combining coefficients for user k and AP l. With MMSE combining, the combining vector of user k $\boldsymbol{v}_k^{\text{sf}}[n] = [\boldsymbol{v}_{kl}[n],\ l \in \mathcal{L}_k]^T$, is given by

$$\boldsymbol{v}_k^{\text{sf}}[n] = p_k \left[\sum_{i=1}^{K} p_i \boldsymbol{h}_{i,\mathcal{L}_k}[n-d] \boldsymbol{h}_{i,\mathcal{L}_k}^H[n-d] + \sigma^2 \boldsymbol{I} \right]^{-1} \times \boldsymbol{h}_{k,\mathcal{L}_k}[n-d], \tag{10}$$

where, $\boldsymbol{h}_{i,\mathcal{L}_k}$ is the vector of NT_k channel gains from the i^{th} user to the set of APs in $\mathcal{L}_k$. Similar to (8) and (9), the average SE and the instantaneous SINR of user k are obtained as follows:

$$\text{SE}_k^{\text{sf}}[n] = \mathbb{E} \log_2(1 + \text{SINR}_k^{\text{sf}}[n]) \tag{11}$$

and

$$\text{SINR}_k^{\text{sf}}[n] = \frac{p_k |\boldsymbol{v}_k^{\text{sf}}[n]^H \boldsymbol{h}_{k,\mathcal{L}_k}[n]|^2}{\sum_{i=1;i\neq k}^{K} p_i |\boldsymbol{v}_k^{\text{sf}}[n]^H \boldsymbol{h}_{i,\mathcal{L}_k}[n]|^2 + \sigma^2 \|\boldsymbol{v}_k^{\text{sf}}[n]\|^2}. \tag{12}$$

Note that (12) reduces to (9) when $M = K$. The algorithm to select the best-M users is given below in Algorithm 1.

V. ANALYTICAL EXPRESSIONS FOR SE IN TERMS OF SPATIAL COVARIANCE MATRICES

In this section, we present a novel and tractable approximation of the expressions for the uplink SE of users. We derive deterministic equivalents of SINR, which are asymptotically tight. The large system limit is considered, i.e., K and L go to infinity while keeping K/L finite. The proposed analytical expressions are 'deterministic' as they depend only on the spatial covariance matrices and not on the small-scale fading coefficients. We first provide some background from random matrix theory before proceeding with the analysis.

Theorem 1 [31, Theorem 3.7]: Let $\boldsymbol{A} \in \mathbb{C}^{N\times N}$ and $\boldsymbol{x}, \boldsymbol{y} \sim \mathcal{CN}(\boldsymbol{0}, \frac{1}{N}\boldsymbol{I}_N)$. Assume that $\boldsymbol{A}$ has uniformly bounded spectral norm (with respect to N), and $\boldsymbol{x}$ and $\boldsymbol{y}$ are mutually independent and independent of $\boldsymbol{A}$. Then, we have

$$\boldsymbol{x}^H \boldsymbol{A} \boldsymbol{x} - \frac{1}{N} tr(\boldsymbol{A}) \xrightarrow[N\to\infty]{a.s} 0, \quad \boldsymbol{x}^H \boldsymbol{A} \boldsymbol{y} \xrightarrow[N\to\infty]{a.s} 0. \tag{13}$$

As shown in Appendix A, we use Theorem 1 to derive a diagonal matrix approximation for $\boldsymbol{H}^H[n]\boldsymbol{H}[n]$, where $\boldsymbol{H}[n] = \left[\sqrt{p_1}\boldsymbol{h}_1[n], \dots, \sqrt{p_K}\boldsymbol{h}_K[n]\right]$, as follows. The $(k,k')^{\text{th}}$ element $\left[\boldsymbol{H}^H[n]\boldsymbol{H}[n]\right]_{k,k'}$ of $\boldsymbol{H}^H[n]\boldsymbol{H}[n]$, for $k, k' = 1, \dots, LN$, is approximated as,

$$\left[\boldsymbol{H}^H[n]\boldsymbol{H}[n]\right]_{k,k'} \approx \begin{cases} p_k \text{tr}(\boldsymbol{R}_k), & \text{for } k = k', \\ 0, & \text{for } k \neq k', \end{cases} \tag{14}$$

where $\boldsymbol{R}_k$ is a block-diagonal matrix with matrices $\boldsymbol{R}_{k1}, \dots, \boldsymbol{R}_{kL}$ along the diagonals. This approximation allows us to derive compact and computationally simpler expressions for average SE unlike the earlier deterministic equivalent results reported in [28] and [32]. We note that similar diagonal matrix approximations have been considered in [11] and [33], and is justified by the fact the channel gain vectors of the users become orthogonal as the number of APs increases to infinity. As can be seen, the off-diagonal coefficients compared to the diagonal coefficients become smaller as L increases. We now present the analytical SE expressions for the cases of perfect CSI ($d = 0$) and outdated CSI ($d > 0$) at the CPU.

A. PERFECT CSI AT CPU (WITHOUT CHANNEL AGING)

For the scenario wherein the CPU has the perfect knowledge of channel conditions, we have the following result for the selective user forwarding scenario. The SE of CF-mMIMO is a generalization of the same.

Result 1: The average SE of user k is approximated as $SE_k \approx \log_2(1+\overline{SINR}_k)$, where $\overline{SINR}_k$ is given by

$$\overline{SINR}_k = \frac{p_k tr(\boldsymbol{R}_{k\mathcal{L}_k})}{\sigma^2} - \frac{p_k}{\sigma^2}\sum_{i=1,i\neq k}^{K}\frac{p_i tr(\boldsymbol{R}_{k\mathcal{L}_k}\boldsymbol{R}_{i\mathcal{L}_k})}{\sigma^2+p_i tr(\boldsymbol{R}_{i\mathcal{L}_k})}, \quad (15)$$

where $\boldsymbol{R}_{k\mathcal{L}_k}$ is the spatial covariance matrix of the k^{th} user to $\mathcal{L}_k$ APs. If we consider $\mathcal{L}_k$ to be set of all APs, L, we get the expressions for CF-mMIMO.

Proof: The proof is given in Appendix B. ■

The $\overline{\text{SINR}}_k$ expression can be easily evaluated given the spatial covariance matrices, transmit powers, and noise variance. The interference experienced by user k from user i is determined by the product matrix $\boldsymbol{R}_{k\mathcal{L}_k}\boldsymbol{R}_{i\mathcal{L}_k}$.

B. OUTDATED CSI AT CPU (WITH CHANNEL AGING)

The SINR expressions with outdated CSI at the CPU are given as follows.

Result 2: The average SE of user k is approximated as $SE_k \approx \log_2(1+\overline{SINR}_k)$, where $\overline{SINR}_k$ is given by $\overline{SINR}_k = S_k/(I_k+N_k)$, where the signal power S_k, interference power I_k, and noise power N_k are given by expressions (16), (17), and (18), as shown at the bottom of the next page.

In the expressions, the constants ϑ_k and ζ_k are given by, $\vartheta_k = \frac{p_k}{\sigma^2+p_k\boldsymbol{R}_{k\mathcal{L}_k}}$, and $\zeta_k = \frac{p_k\sigma^2}{\sigma^2+p_k\text{tr}(\boldsymbol{R}_{k\mathcal{L}_k})-p_k\sum_{i=1;i\neq k}^{K}\frac{p_i\text{tr}\boldsymbol{R}_{k\mathcal{L}_k}\boldsymbol{R}_{i\mathcal{L}_k}}{\sigma^2+p_i\text{tr}\left(\boldsymbol{R}_{i\mathcal{L}_k}\right)}}$, where k denotes the user index.

Proof: The proof is given in Appendix C. ■

Note that the analytic expressions for CF-mMIMO can be obtained from the expressions of selective user forwarding by considering $LN \times LN$ spatial covariance matrix of all the K users instead of best-M users in the analysis.

VI. NUMERICAL RESULTS AND ANALYSIS

In this section, we first describe the simulation setup and then provide the simulation results and insights into the results for different system parameters and configurations.

A. SIMULATION SETUP

We consider a 1 km × 1 km network area with uniformly distributed APs in it. Each AP is assumed to be at a height of 10 m above the ground. We consider 3GPP Urban Micro-cell model [30, Table B 1.2.1] with 2GHz carrier frequency. The large-scale fading coefficients between k^{th} UE and l^{th} AP is generated using equation (2). We assume that all the users transmit with equal power $p_k = 100$ mW over the bandwidth of 20 MHz, and the noise power is $\sigma^2 = -96$ dBm.

B. SIMULATION RESULTS AND DISCUSSIONS

We first discuss the fronthaul signaling computations for the proposed scheme and compare its performance with a user-centric scheme DCC [3]. In DCC, the criterion for UE-AP clustering is the number of orthogonal pilot carriers. We then study the SE analysis of the proposed scheme for different system configurations.

1) FRONTHAUL SIGNALING COMPUTATIONS

In the selective user forwarding scheme, the total fronthaul signaling will be $KLN + ML + MLN$ complex symbols for channel estimation and combining vector computation in each coherence interval and ML complex symbols in each symbol time. When $K = M$, the original CF-mMIMO signaling is obtained. Substituting the value of M, L, and N, we see that, the selective forwarding scheme gives a fronthaul savings of 77.5%, 62.5% and 50% for $M = 9$, $M = 15$ and $M = 20$ respectively. In the DCC scheme, each AP can serve at most $|\tau_p|$ users. Hence the total fronthaul signaling would be $|\tau_p|LN + |\tau_p|LN$. Here $|\tau_p|$ is the number of orthogonal pilot carriers. In one coherence interval and $|\tau_p|L$ complex symbols in each symbol time.

Experiment 1: In this experiment we compare the performance of selective user forwarding with the DCC scheme for different values of M as, $M = 9$, and $M = 15$ for a $|\tau_p|$ value of 10. Other system parameters are $L = 100$, $N = 4$, $K = 40$ and $\rho = 0.8$.

The performance comparison of the DCC scheme with the selective forwarding scheme is given in Fig. 4, both for perfect and outdated CSI. For the case of perfect CSI, in the 90% likely SE regions, the relative drop in SE compared to the conventional CF-mMIMO is 5.2% for selective user forwarding (with $M = 9$) and 13.37% for DCC scheme (with $|\tau_p| = 10$). For the scenario, where the combining is based on delayed CSI, the performance is almost similar for both of the schemes. Also, as the M value increases, the SE performance of CF-mMIMO with selective user forwarding gets close to the conventional CF-mMIMO case. We see that, for $M = 15$, the performance is almost similar to the CF-mMIMO with more than 60% savings in fronthaul signaling. Also, when $M = 9$ and $\tau_p = 10$, selective user forwarding yields better performance than DCC scheme for the case of perfect CSI.

Experiment 2: In this experiment we study the variation of SE with the number of antennas, N, at each AP. We study two cases when $N = 1$ and $N = 16$. This experiment also tries to analyze the effect of imperfect β_{kl} values on SE, which can happen due to the mobility of the UEs, for selective user forwarding. We consider the case for $M = 9$, $L = 100$, $K = 40$, $\rho = 0.8$.

As evident from Fig. 5, the performance improves significantly with the number of antennas both for perfect CSI and imperfect CSI. This trend holds true for both conventional CF-mMIMO and CF-mMIMO with selective user forwarding. For instance, in the 90% likely SE regions, there is a 41.47% relative increase in the SE for perfect CSI. In the

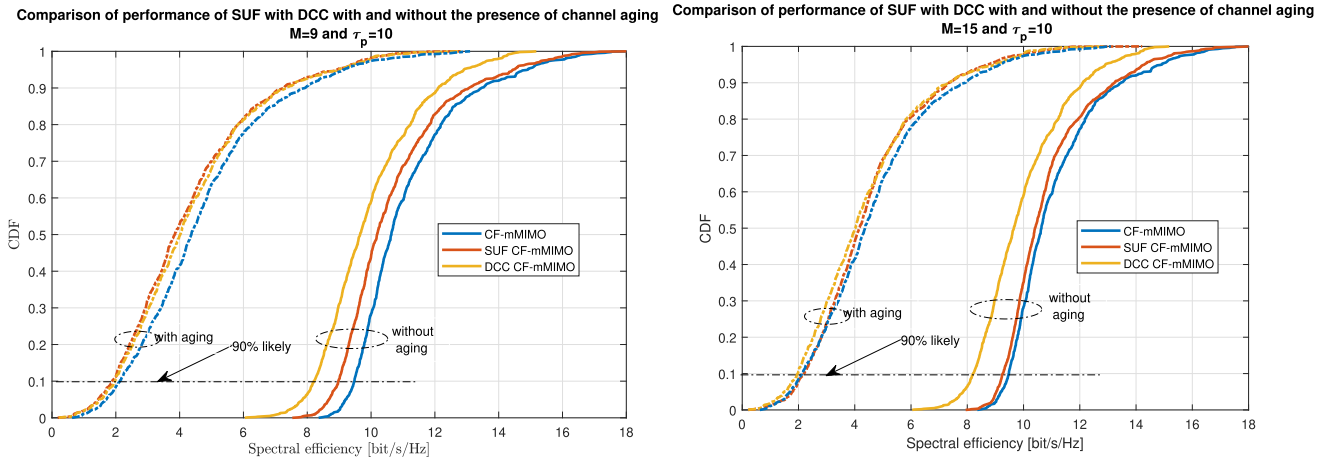

(a) $M = 9$ and $|\tau_p| = 10$ (b) $M = 15$ and $|\tau_p| = 10$

FIGURE 4. SE performance comparison with outdated combining vector for selective user forwarding (SUF) and DCC, and for (a) $M = 9$ (b) $M = 15$.

case of outdated CSI, there is a performance improvement of 60.06%. A similar trend is also observed for selective user forwarding case. This is because, as the value of N increases, the number of antennas available for coherent combining in the uplink also increases leading to better performance in the presence or absence of perfect CSI.

The same figure also shows the effect of imperfect β_{kl} values due to mobility in the SE performance. We consider the case when each β_{kl} value is affected by a $\Delta\beta_{kl}$ value of relative variance 20% of the original β_{kl} value. Even then, from the figure, it is evident that the performance of the system is not significantly impacted.

$$
\begin{aligned}
S_k = p_k\zeta_k^2\Bigg[&|\rho|^2\,\mathrm{tr}^2(\boldsymbol{R}_{k\mathcal{L}_k}) + (1-|\rho|^2)\,\mathrm{tr}(\boldsymbol{R}_{k\mathcal{L}_k}^2) - \sum_{m\neq k}\vartheta_m\Big[|\rho|^2\,\mathrm{tr}(\boldsymbol{R}_{k\mathcal{L}_k})\,\mathrm{tr}(\boldsymbol{R}_{k\mathcal{L}_k}\boldsymbol{R}_{m\mathcal{L}_k}) + (1-|\rho|^2)\,\mathrm{tr}(\boldsymbol{R}_{k\mathcal{L}_k}^2\boldsymbol{R}_{m\mathcal{L}_k})\Big] \\
&- \sum_{r\neq k}\vartheta_r\Big[|\rho|^2\,\mathrm{tr}(\boldsymbol{R}_{k\mathcal{L}_k}\boldsymbol{R}_{r\mathcal{L}_k})\,\mathrm{tr}(\boldsymbol{R}_{k\mathcal{L}_k}) + (1-|\rho|^2)\,\mathrm{tr}(\boldsymbol{R}_{k\mathcal{L}_k}^2\boldsymbol{R}_{r\mathcal{L}_k})\Big] + \sum_{m\neq k}\sum_{r\neq k}\vartheta_r\vartheta_m\Big[|\rho|^2\,\mathrm{tr}(\boldsymbol{R}_{k\mathcal{L}_k}\boldsymbol{R}_{r\mathcal{L}_k})\,\mathrm{tr}(\boldsymbol{R}_{k\mathcal{L}_k}\boldsymbol{R}_{m\mathcal{L}_k}) \\
&+ (1-|\rho|^2)\,\mathrm{tr}(\boldsymbol{R}_{k\mathcal{L}_k}^2\boldsymbol{R}_{m\mathcal{L}_k}\boldsymbol{R}_{r\mathcal{L}_k})\mathbb{1}_{\{r\neq m\}}\Big] + \sum_{r\neq k}\vartheta_r^2\,\mathrm{tr}^2(\boldsymbol{R}_{r\mathcal{L}_k}\boldsymbol{R}_{k\mathcal{L}_k})\mathbb{1}_{\{r=m\}}\Bigg].
\end{aligned}
\tag{16}
$$

$$
\begin{aligned}
I_k = \zeta_k^2\sum_{i\neq k}p_i(\mathrm{tr}(\boldsymbol{R}_{k\mathcal{L}_k}\boldsymbol{R}_{i\mathcal{L}_k}) &- \vartheta_m\Big[|\rho|^2\,\mathrm{tr}(\boldsymbol{R}_{k\mathcal{L}_k}\boldsymbol{R}_{i\mathcal{L}_k})\,\mathrm{tr}(\boldsymbol{R}_{i\mathcal{L}_k}) + (1-|\rho|^2)\,\mathrm{tr}(\boldsymbol{R}_{i\mathcal{L}_k}^2\boldsymbol{R}_{k\mathcal{L}_k})\Big]\mathbb{1}_{\{i=m\}} \\
&- \sum_{m\neq k}\vartheta_m\,\mathrm{tr}(\boldsymbol{R}_{k\mathcal{L}_k}\boldsymbol{R}_{i\mathcal{L}_k}\boldsymbol{R}_{m\mathcal{L}_k})\mathbb{1}_{\{i\neq m\}} - \vartheta_r\Big[|\rho|^2\,\mathrm{tr}(\boldsymbol{R}_{r\mathcal{L}_k})\,\mathrm{tr}(\boldsymbol{R}_{r\mathcal{L}_k}\boldsymbol{R}_{k\mathcal{L}_k}) + (1-|\rho|^2)\,\mathrm{tr}(\boldsymbol{R}_{k\mathcal{L}_k}\boldsymbol{R}_{r\mathcal{L}_k}^2)\Big]\mathbb{1}_{\{r=i\}} \\
&- \sum_{r\neq k}\mathrm{tr}(\boldsymbol{R}_{k\mathcal{L}_k}\boldsymbol{R}_{r\mathcal{L}_k}\boldsymbol{R}_{i\mathcal{L}_k})\mathbb{1}_{\{r\neq i\}} + \sum_{i\neq k}\vartheta_i^2\Big[|\rho|^2\,\mathrm{tr}(\boldsymbol{R}_{k\mathcal{L}_k}\boldsymbol{R}_{i\mathcal{L}_k})\,\mathrm{tr}^2(\boldsymbol{R}_{i\mathcal{L}_k}^{0.5}) + (1-|\rho|^2)\,\mathrm{tr}(\boldsymbol{R}_{k\mathcal{L}_k}\boldsymbol{R}_{i\mathcal{L}_k})\,\mathrm{tr}(\boldsymbol{R}_{i\mathcal{L}_k}^2)\Big]\mathbb{1}_{\{i=r=m\}} \\
&+ \sum_{m\neq k}\vartheta_m^2\,\mathrm{tr}(\boldsymbol{R}_{m\mathcal{L}_k}\boldsymbol{R}_{i\mathcal{L}_k})\,\mathrm{tr}(\boldsymbol{R}_{m\mathcal{L}_k}\boldsymbol{R}_{k\mathcal{L}_k})\mathbb{1}_{\{m=r\neq i\}} + \sum_{m\neq k}\vartheta_m\vartheta_i\Big[|\rho|^2\,\mathrm{tr}(\boldsymbol{R}_{i\mathcal{L}_k})\,\mathrm{tr}(\boldsymbol{R}_{i\mathcal{L}_k}\boldsymbol{R}_{m\mathcal{L}_k}\boldsymbol{R}_{k\mathcal{L}_k}) \\
&+ (1-|\rho|^2)\,\mathrm{tr}(\boldsymbol{R}_{i\mathcal{L}_k}^2\boldsymbol{R}_{m\mathcal{L}_k}\boldsymbol{R}_{k\mathcal{L}_k})\Big]\mathbb{1}_{\{m\neq r=i\}} \\
&+ \sum_{r\neq k}\vartheta_r\vartheta_i\Big[|\rho|^2\,\mathrm{tr}(\boldsymbol{R}_{i\mathcal{L}_k})\,\mathrm{tr}(\boldsymbol{R}_{i\mathcal{L}_k}\boldsymbol{R}_{k\mathcal{L}_k}\boldsymbol{R}_{r\mathcal{L}_k}) + (1-|\rho|^2)\,\mathrm{tr}(\boldsymbol{R}_{i\mathcal{L}_k}^2\boldsymbol{R}_{k\mathcal{L}_k}\boldsymbol{R}_{r\mathcal{L}_k})\Big]\mathbb{1}_{\{m=i\neq r\}} \\
&+ \sum_{m\neq k}\sum_{r\neq k}\vartheta_r\vartheta_m\,\mathrm{tr}(\boldsymbol{R}_{k\mathcal{L}_k}\boldsymbol{R}_{r\mathcal{L}_k}\boldsymbol{R}_{i\mathcal{L}_k}\boldsymbol{R}_{m\mathcal{L}_k})\mathbb{1}_{\{i\neq r\neq m\}}).
\end{aligned}
\tag{17}
$$

$$
\begin{aligned}
N_k = \mathrm{tr}(\boldsymbol{R}_{k\mathcal{L}_k}) - \sum_{m\neq k}\vartheta_m\,\mathrm{tr}(\boldsymbol{R}_{k\mathcal{L}_k}\boldsymbol{R}_{m\mathcal{L}_k}) - \sum_{r\neq k}\vartheta_r\,\mathrm{tr}(\boldsymbol{R}_{k\mathcal{L}_k}\boldsymbol{R}_{r\mathcal{L}_k}) + \sum_{m\neq k}\vartheta_m^2\,\mathrm{tr}(\boldsymbol{R}_{m\mathcal{L}_k}\boldsymbol{R}_{k\mathcal{L}_k})\,\mathrm{tr}(\boldsymbol{R}_{m\mathcal{L}_k})\mathbb{1}_{\{m=r\}} \\
+ \sum_{r\neq k}\sum_{m\neq k}\vartheta_r\vartheta_m\,\mathrm{tr}(\boldsymbol{R}_{k\mathcal{L}_k}\boldsymbol{R}_{r\mathcal{L}_k}\boldsymbol{R}_{m\mathcal{L}_k})\mathbb{1}_{\{m\neq r\}},
\end{aligned}
\tag{18}
$$

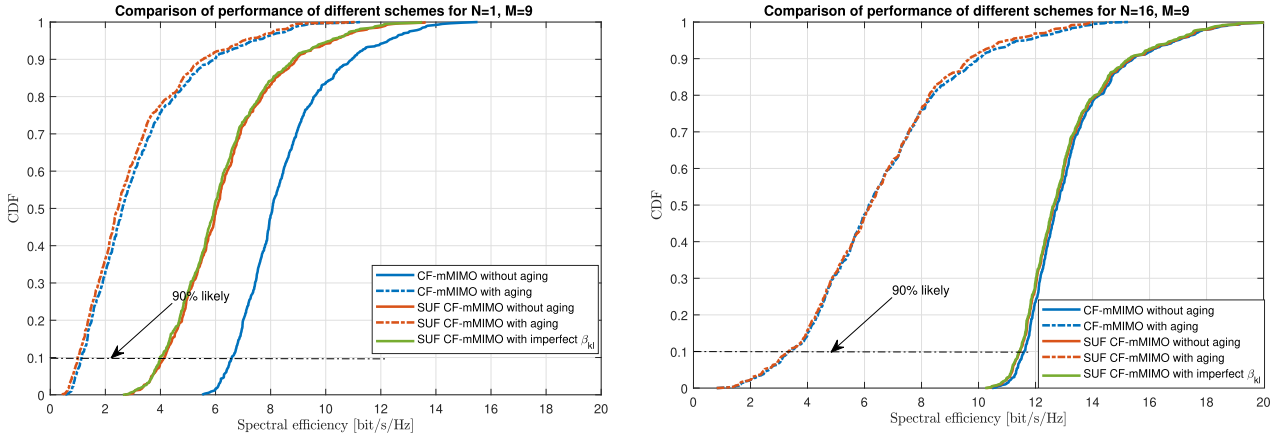

(a) $M = 9$ and $N = 1$ (b) $M = 9$ and $N = 16$

FIGURE 5. SE performance comparison with different number of antennas at each AP, N, and imperfect β_{kl} values.

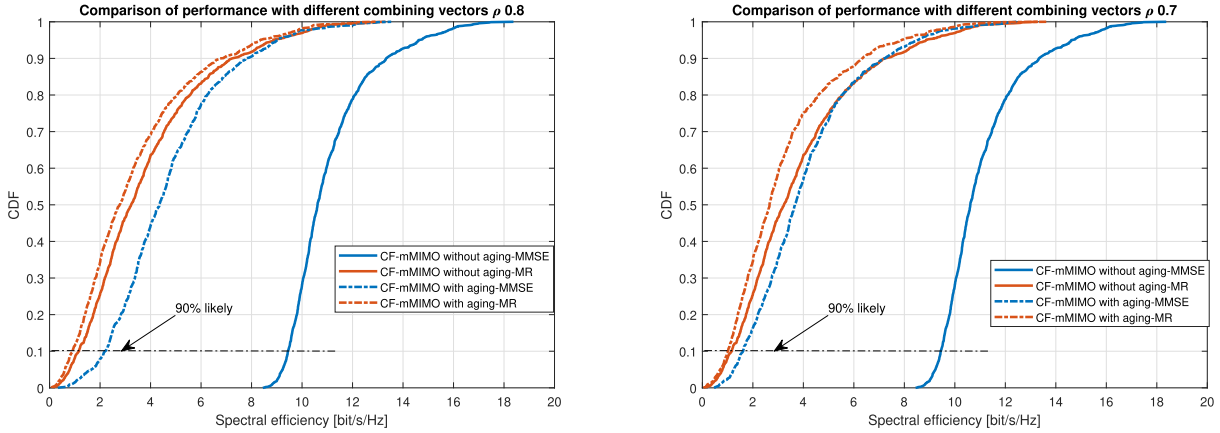

(a) $\rho = 0.8$ (b) $\rho = 0.7$

FIGURE 6. SE performance comparison with perfect and outdated combining for (a) $\rho = 0.8$ (b) $\rho = 0.7$ for MMSE and MR combining.

This in-turn shows that, for selective user forwarding, the relative magnitude of large-scale fading coefficients is relevant and not their absolute value. This is because the AP selects M users with the largest large-scale fading coefficient values.

Experiment 3: In this experiment, we try to compare the performance of two combining schemes for uplink. We consider maximum ratio (MR) combining and compare it with MMSE combining for $\rho = 0.8$ *and* $\rho = 0.7$. *We consider* $L = 100$, $N = 4$, $K = 40$ *and* $M = 9$.

In the uplink of CF-mMIMO, we evaluate the performance of MMSE combining and compare it with MR combining in the presence of both perfect and outdated CSI. Note that MR combining is employed to maximize the signal-to-noise ratio (SNR). For MR combining, the combining vector for the k^{th} UE is $\boldsymbol{v}_k[n] = \boldsymbol{h}_k[n]$, when perfect CSI is available at the CPU, and $\boldsymbol{v}_k[n] = \boldsymbol{h}_k[n-d]$, when only delayed CSI is available.

Fig. 6 illustrates the performance comparison of MR and MMSE combining schemes. It is observed that MR combining performs poorly even under perfect CSI scenarios. For instance, when $\rho = 0.8$, in the 90% likely SE regions, the SE is 1.42 bits/s/Hz which decreases to 0.898 bits/s/Hz due to channel aging. As the ρ value decreases, the performance becomes worse with delayed CSI. On the other hand, under perfect CSI, the 90% likely SE of MMSE combining vector is around 9 bits/s/Hz. Hence MMSE combining clearly outperforms MR combining and is used in our analysis.

Experiment 4: In this experiment, we study the accuracy of the derived analytical expressions for different number of antennas and for different temporal coefficient values, ρ. *We consider,* $N = 4$, $K = 40$ *and* $M = 9$.

Fig. 7, shows the performance of CF-mMIMO with selective user forwarding for both perfect and outdated CSI using only the analytical expressions. From the figure, it is evident that for selective user forwarding, the performance curves,

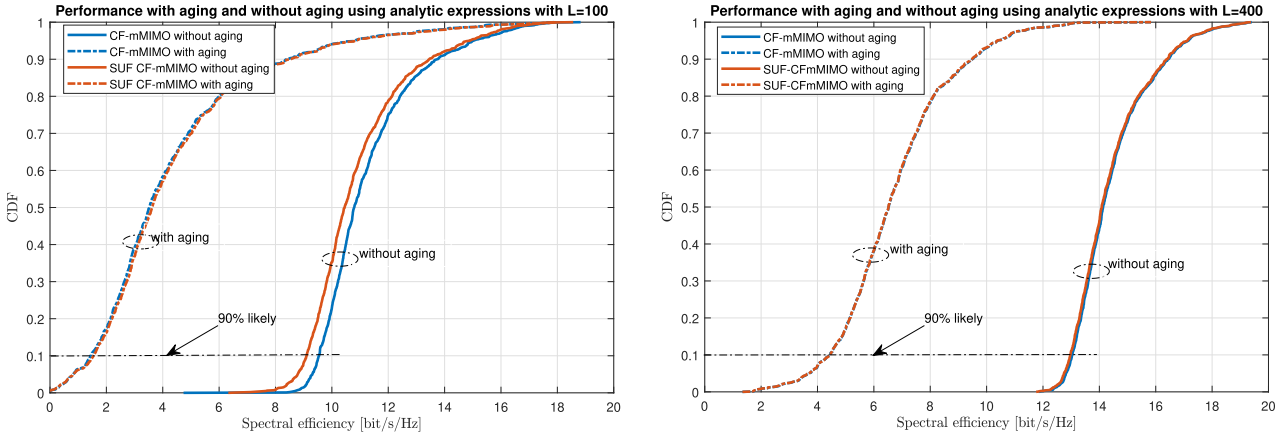

(a) $L = 100$ and $N = 4$ (b) $L = 400$ and $N = 4$

FIGURE 7. SE performance comparison for perfect and outdated combining using analytical expressions for different number of APs (L). For SUF scheme, $M = 9$ is assumed.

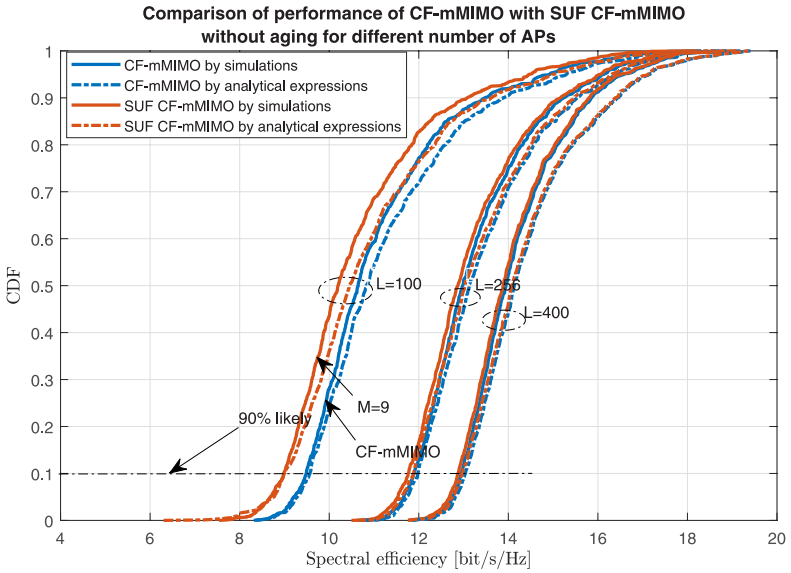

FIGURE 8. SE performance comparison of CF-mMIMO with selective user forwarding(with M=9) under perfect CSI and for different number of APs, L.

become very close to the conventional CF-mMIMO, as the system dimension is increased. Also, the loss in system performance due to outdated CSI can be quantified using analytic curves.

In Fig. 8, CDF of the SE for a random user in CF-mMIMO with and without the selective user forwarding for the perfect CSI scenario is plotted for $L = 100$, $L = 256$, and $L = 400$. It also depicts the tightness of the analytical expressions. We see that when the number of APs increases, the performance of the CF-mMIMO system is improving significantly. This is due to the increase in macro-diversity as a result of the increase in the number of distributed APs, which in turn yields SE performance gains. The same trend is observed in selective user forwarding scenarios. Also, for the 90% likely regions, the relative drop in SE when only selected users data are forwarded decreases as the number of APs in the network increases. For example, in the 90% likely SE regions, when $L = 100$, the drop in SE is 5.2%, whereas it reduces significantly to 1.2% and 0.5% for $L = 256$ and $L = 400$ respectively.

Also, from Fig. 8, we can see that the derived analytical expressions have an excellent match in the perfect CSI case. For example, in the 90% likely SE scenarios, the relative difference is only 0.9% for $L = 100$ and is very negligible for $L = 256$ and $L = 400$. We note that the analytical approximation for the conventional CF-mMIMO is much tighter than the selective user forwarding case since the accuracy of the diagonal approximation improves as the system dimension increases. Also, recall that these expressions solely rely on the spatial covari-

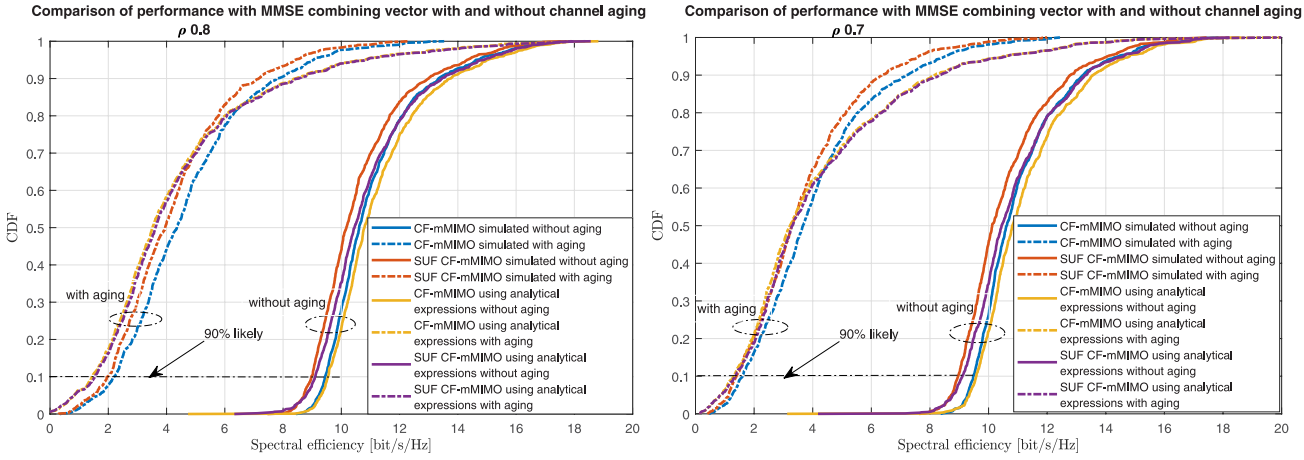

(a) $\rho = 0.8$ (b) $\rho = 0.7$

FIGURE 9. SE performance with outdated combining vector for different correlation coefficient (ρ) values.

ance matrices, thereby enabling the quantification of system performance without requiring knowledge of instantaneous channel gains.

Fig. 9 depicts the comparison of SE for different values of ρ, for CF-mMIMO with and without selective user forwarding. Several observations can be found from the results. First, there is a significant degradation in SE when the combining vector is computed using the delayed CSI. For example, for a correlation coefficient $\rho = 0.8$, in the 90% likely SE regions, there is a drop of 76.9% in the CF-mMIMO case. This shows that having outdated CSI severely impacts the system performance. Also, it can be seen that as the ρ value increases, the curves for outdated combining move towards the right. For example, in the 90% likely regions, the SE drop is 83.13%, and 77.12% for a correlation coefficient of 0.7, and 0.8, respectively, for the conventional CF-mMIMO case. Second, we can observe that the analytical expressions are quite accurate in predicting the behavior of the system for both perfect and delayed CSI scenarios. Hence, as can be seen, the proposed analytical expressions act as an effective and accurate tool to characterize the performance of the CF-mMIMO systems of large sizes.

Third, for the system with selective user forwarding, the performance with outdated combining vector is almost similar to that of the general CF-mMIMO case. There is a significant drop in performance as the channel becomes outdated. For example, in the 90% likely SE regions, the relative drop in SE is 83.13%, and 77.2% for ρ values of 0.7, and 0.8 respectively.

VII. CONCLUSION

In this paper, we proposed a selective user forwarding scheme and studied its performance under channel aging. In the proposed scheme, the data of only a subset of UEs are forwarded to the CPU in the uplink. This approach enabled the deterministic design of the fronthaul as the number of UEs served by each AP is fixed. Also, we have shown that the selective user forwarding approach yields significant savings in fronthaul signaling with negligible loss in SE compared to the conventional CF-MIMO scheme. The performance of the selective user forwarding scheme has been evaluated in different scenarios (e.g., with perfect and outdated CSI scenarios) and for various system parameters, such as correlation coefficients, system dimensions, etc. Moreover, it is shown that the derived analytical expressions are accurate, and therefore due to their simplicity of use, they can be employed as an effective and easy-to-use design tool for the performance characterization of future CF-mMIMO systems that may have arbitrarily high dimensions. Analyzing the SE using Monte-Carlo expressions for such systems would be computationally complex.

Future efforts will involve extending this design framework for CF-mMIMO downlink and formulating practical optimization problems for finding the optimal set of APs to which a particular UE gets associated to. Optimizing the set of UEs associated with an AP subject to the maximum number of UEs can also be an avenue for future research

APPENDIX A
DIAGONAL MATRIX APPROXIMATION

The $(k,k)^{\text{th}}$ element of $\boldsymbol{H}^H[n]\boldsymbol{H}[n]$ is $p_k\boldsymbol{h}_k^{\text{H}}[n]\boldsymbol{h}_k[n]$, for $k = 1,\ldots,LN$. Since $\boldsymbol{h}_k[n] \sim \boldsymbol{R}_k^{1/2}\boldsymbol{x}_k[n]$, where $\boldsymbol{x}_k[n] \sim \mathcal{CN}(\boldsymbol{0},\boldsymbol{I})$, we have $\boldsymbol{h}_k^{\text{H}}[n]\boldsymbol{h}_k[n] = \boldsymbol{x}_k^H[n]\boldsymbol{R}_k\boldsymbol{x}_k[n]$. Further, using Theorem 1, we get $\boldsymbol{h}_k^{\text{H}}[n]\boldsymbol{h}_k[n] \approx \text{tr}(\boldsymbol{R}_k)$.

Now, we consider the $(k,k')^{\text{th}}$ element of $\boldsymbol{H}^H[n]\boldsymbol{H}[n]$ for $k \neq k'$. It is given by $\sqrt{p_k p_{k'}}\boldsymbol{h}_k^{\text{H}}[n]\boldsymbol{h}_{k'}[n]$. As before, $\boldsymbol{h}_k^{\text{H}}[n]\boldsymbol{h}_{k'}[n] = \boldsymbol{x}_k^{\text{H}}[n]\boldsymbol{R}_k^{1/2}\boldsymbol{R}_{k'}^{1/2}\boldsymbol{x}_{k'}[n]$. Since $\boldsymbol{h}_k[n]$ and $\boldsymbol{h}_{k'}[n]$ are mutually independent, using Theorem 1, we get $\boldsymbol{h}_k^{\text{H}}[n]\boldsymbol{h}_{k'}[n] \approx 0$.

Using the above approximations for $\boldsymbol{h}_k^{\text{H}}[n]\boldsymbol{h}_k[n]$ and $\boldsymbol{h}_k^{\text{H}}[n]\boldsymbol{h}_{k'}[n]$, we get (14). The (k,k) element of $\boldsymbol{H}^{\text{H}}[n]\boldsymbol{H}[n]$ converges to tr $(\boldsymbol{R}_k)$ and (k,k') element to zero.

APPENDIX B
SINR EXPRESSIONS FOR PERFECT CSI SCENARIO

Here, we derive SINR for the general CF-mMIMO systems in the perfect CSI scenario. The instantaneous SINR with perfect CSI can be simplified as,

$$\mathrm{SINR}_k[n] = p_k \boldsymbol{h}_k^{\mathrm{H}}[n] \left(\boldsymbol{H}_{\setminus k}[n] \boldsymbol{H}_{\setminus k}^{\mathrm{H}}[n] + \sigma^2 \boldsymbol{I}_{LN} \right)^{-1} \boldsymbol{h}_k[n], \tag{19}$$

where, $\boldsymbol{H}_{\setminus k}[n]$ is a $(K-1)\times(K-1)$ dimension matrix of the channel gains of all the users excluding the k^{th} user. Applying the Woodbury Inversion lemma [34, 2.1.3] in equation (19), we have,

$$\begin{aligned}\mathrm{SINR}_k[n] = {} & p_k \boldsymbol{h}_k^{\mathrm{H}}[n] \boldsymbol{h}_k[n] \\ & - p_k \boldsymbol{h}_k^{\mathrm{H}}[n] \boldsymbol{H}_{/k}[n] \left(\boldsymbol{I}_{K-1} + \boldsymbol{H}_{/k}^{\mathrm{H}}[n] \boldsymbol{H}_{/k}[n] \right)^{-1} \\ & \times \boldsymbol{H}_{\setminus k}^{\mathrm{H}}[n] \boldsymbol{h}_k[n].\end{aligned} \tag{20}$$

For $k = k'$, we have

$$\begin{aligned}\boldsymbol{h}_k^{\mathrm{H}}[n] \boldsymbol{h}_k[n] & \xrightarrow[Distribution]{In} \boldsymbol{x}^{\mathrm{H}}[n] \boldsymbol{R}_{\boldsymbol{k}} \boldsymbol{x}_k[n],\ \boldsymbol{x}_k[n] \sim \mathcal{CN}(\boldsymbol{0}, \boldsymbol{I}_{LN}) \\ & \xrightarrow{\text{Theorem 1}} \mathrm{tr}(\boldsymbol{R}_k).\end{aligned} \tag{21}$$

For $k \neq k'$, note that we can write

$$\begin{bmatrix} \boldsymbol{h}_k[n] \\ \boldsymbol{h}_{k'}[n] \end{bmatrix} = \begin{bmatrix} \boldsymbol{R}_k & \boldsymbol{0} \\ \boldsymbol{0} & \boldsymbol{R}_{k'} \end{bmatrix}^{0.5} \begin{bmatrix} \boldsymbol{x}_k[n] \\ \boldsymbol{y}_k[n] \end{bmatrix},$$
$$\boldsymbol{x}_k[n], \boldsymbol{y}_k[n] \sim \mathcal{CN}(\boldsymbol{0}, \boldsymbol{I}_{LN}).$$

we have,

$$\boldsymbol{h}_k^{\mathrm{H}}[n] \boldsymbol{h}_{k'}[n] \xrightarrow{Theorem1} 0. \tag{22}$$

Based on (21) and (22), we have,

$$\left(\boldsymbol{I}_{K-1} + \boldsymbol{H}_{/k}^{\mathrm{H}}[n] \boldsymbol{H}_{/k}[n] \right)^{-1} \approx \mathrm{diag} \left\{ \frac{1}{1 + p_{k'} \mathrm{tr} \boldsymbol{R}_{k'}} \right\}_{k' \neq k}. \tag{23}$$

Substituting in (20), we get

$$\mathrm{SINR}_k[n] = p_k \boldsymbol{h}_k[n] \boldsymbol{h}_k^{\mathrm{H}}[n] - p_k \sum_{k \neq k'} \frac{p_{k'} |\boldsymbol{h}_k^{\mathrm{H}}[n] \boldsymbol{h}_{k'}[n]|^2}{1 + p_{k'} \mathrm{tr}(\boldsymbol{R}_{k'})} \tag{24}$$

Considering the numerator,

$$\begin{aligned}& \left| \boldsymbol{h}_k^{\mathrm{H}}[n] \boldsymbol{h}_{k'}[n] \right|^2 \\ & = \boldsymbol{h}_k^{\mathrm{H}}[n] \boldsymbol{h}_{k'}[n] \boldsymbol{h}_{k'}^{\mathrm{H}}[n] \boldsymbol{h}_k[n] \\ & \xrightarrow[Distribution]{In} \boldsymbol{x}_k^{\mathrm{H}}[n] \boldsymbol{R}_k^{0.5} \boldsymbol{R}_{k'}^{0.5} \boldsymbol{x}_{k'}[n] \boldsymbol{x}_{k'}^{\mathrm{H}}[n] \boldsymbol{R}_{k'}^{0.5} \boldsymbol{R}_k^{0.5} \boldsymbol{x}_k[n] \\ & \xrightarrow{Theorem1} \mathrm{tr}\left(\boldsymbol{R}_k \boldsymbol{R}_{k'}^{0.5} \boldsymbol{x}_{k'}[n] \boldsymbol{x}_{k'}^{\mathrm{H}}[n] \boldsymbol{R}_{k'}^{0.5} \right) \\ & \xrightarrow[Distribution]{In} \boldsymbol{x}_{k'}^{\mathrm{H}}[n] \boldsymbol{R}_{k'}^{0.5} r \boldsymbol{R}_k \boldsymbol{R}_{k'}^{0.5} \boldsymbol{x}_{k'}[n] \\ & \xrightarrow{Theorem1} \mathrm{tr}(\boldsymbol{R}_k \boldsymbol{R}_{k'}).\end{aligned} \tag{25}$$

Substituting in (20), we get the desired expression for the numerator.

APPENDIX C
APPROXIMATION FOR THE OUTDATED COMBINING

The outdated combining vector is computed from the delayed channel gains and can be given as

$$\begin{aligned}\boldsymbol{v}_k[n] = p_k \Big(& \boldsymbol{H}_{\setminus k}[n-d] \boldsymbol{H}_{\setminus k}^{\mathrm{H}}[n-d] \\ & + p_k \boldsymbol{h}_k[n-d] \boldsymbol{h}_k^{\mathrm{H}}[n-d] \sigma^2 \boldsymbol{I}_{LN} \Big)^{-1} \boldsymbol{h}_k[n-d]\end{aligned} \tag{26}$$

Using the matrix inversion lemma [35, Lemma 1], we get

$$\boldsymbol{v}_k[n] = \frac{p_k \boldsymbol{\Omega}^{-1}[n-d] \boldsymbol{h}_k[n-d]}{1 + p_k \left(\boldsymbol{h}_k[n-d] \right)^{\mathrm{H}} \boldsymbol{\Omega}^{-1}[n-d] \boldsymbol{h}_k[n-d]},$$

where $\boldsymbol{\Omega}[n-d] = \boldsymbol{H}_{\setminus k}[n-d] \boldsymbol{H}_{\setminus k}^{\mathrm{H}}[n-d] + \sigma^2 \boldsymbol{I}_{LN}$, then $\boldsymbol{\Omega}^{-1}[n-d]$,

$$\begin{aligned}\boldsymbol{\Omega}^{-1}[n-d] = {} & \frac{\boldsymbol{I}_{LN}}{\sigma^2} - \frac{\boldsymbol{H}_{\setminus k}[n-d]}{\sigma^2} \\ & \times \left(\frac{\boldsymbol{H}_{\setminus k}^{\mathrm{H}}[n-d] \boldsymbol{H}_{\setminus k}[n-1]}{\sigma^2} + \boldsymbol{I}_{k-1} \right)^{-1} \\ & \times \frac{\boldsymbol{H}_{\setminus k}[n-d]}{\sigma^2}.\end{aligned}$$

Using diagonal approximation for $\boldsymbol{H}_{\setminus k}^{\mathrm{H}}[n-d] \boldsymbol{H}_{\setminus k}[n-d] = \mathrm{diag}(\mathrm{tr}(\boldsymbol{R})_i)_{i=1,\ldots K; i \neq k}$, we will get

$$\boldsymbol{\Omega}^{-1}[n-d] = \boldsymbol{I}_{LN} - \sum_{i=1; i \neq k}^{K} \frac{p_i \boldsymbol{h}_i[n-d] \boldsymbol{h}_i^H[n-d]}{\sigma^2 \left(1 + \frac{p_i \mathrm{tr}(R)_i}{\sigma^2} \right)},$$

and substituting in the expression for $\boldsymbol{v}_k$ and simplifying the denominator, we get,

$$\begin{aligned}\boldsymbol{v}_k[n] = {} & p_k / \left(1 + \frac{p_k \mathrm{tr}(\boldsymbol{R}_k)}{\sigma^2} - p_k \sum_{i=1; i \neq k}^{K} \frac{p_i \mathrm{tr}(\boldsymbol{R}_k) \boldsymbol{R}_i}{\sigma^2 \left(\sigma^2 + p_i \mathrm{tr}(\boldsymbol{R}_i) \right)} \right) \\ & \times \boldsymbol{\Omega}^{-1}[n-d] \boldsymbol{h}_k[n-d].\end{aligned}$$

i.e.,

$$\boldsymbol{v}_k[n] = \zeta \boldsymbol{\Omega}^{-1}[n-d] \boldsymbol{h}_k[n-d]. \tag{27}$$

Now, instantaneous SINR of the k^{th} user when using the outdated combining vector can be expressed as,

$$\begin{aligned}& \overline{\mathrm{SINR}}_k[n] \\ & = \frac{p_k \boldsymbol{v}_k^{\mathrm{H}}[n] \boldsymbol{h}_k[n] \boldsymbol{h}_k^{\mathrm{H}}[n] \boldsymbol{v}_k[n]}{\sum_{i=1; i \neq k}^{K} p_i \boldsymbol{v}_k^{\mathrm{H}}[n] \boldsymbol{h}_i[n] \boldsymbol{h}_i^{\mathrm{H}}[n] \boldsymbol{v}_k[n] + \sigma^2 \boldsymbol{v}_k^{\mathrm{H}}[n] \boldsymbol{v}_k[n]}\end{aligned}$$

Substituting the value of (27) in the numerator of SINR expression, we get the numerator of SINR expression as $p_k |\zeta|^2 \boldsymbol{h}_k^{\mathrm{H}}[n-d] \boldsymbol{\Omega}^{-1}[n-d] \boldsymbol{h}_k[n] \boldsymbol{h}_k^{\mathrm{H}}[n] \boldsymbol{\Omega}^{-1}[n-d] \boldsymbol{h}_k[n-d]$. Substituting the value of $\boldsymbol{\Omega}^{-1}$ and simplifying we get the numerator of $\overline{\mathrm{SINR}}_k[n]$, $\overline{\mathrm{SINR}}_k^{\mathrm{Nr}}[n]$ as,

$$\overline{\mathrm{SINR}}_k^{\mathrm{Nr}}[n] = \boldsymbol{h}_k^{\mathrm{H}}[n-d] \boldsymbol{h}_k[n] \boldsymbol{h}_k^{\mathrm{H}}[n] \boldsymbol{\Omega}^{-1} \boldsymbol{h}_k[n-d]$$

$$- \sum_{r \neq k} \vartheta_r \boldsymbol{h}_k^{\mathrm{H}}[n-d]\boldsymbol{h}_r[n-d] \times \boldsymbol{h}_r^{\mathrm{H}}[n-d]\boldsymbol{h}_k[n]\boldsymbol{h}_k^{\mathrm{H}}[n]\boldsymbol{\Omega}^{-1}\boldsymbol{h}_k[n-d]. \quad (28)$$

where $\vartheta_r = p_r / \left(\sigma^2 + p_r \operatorname{tr}(\boldsymbol{R}_r)\right)$. Substituting the expression for $\boldsymbol{\Omega}^{-1}[n-d]$, we get,

$$\begin{aligned}
&\overline{\mathrm{SINR}}_k^{\mathrm{Nr}}[n] \\
&= \boldsymbol{h}_k^{\mathrm{H}}[n-d]\boldsymbol{h}_k[n]\boldsymbol{h}_k^{\mathrm{H}}[n]\boldsymbol{h}_k[n-d] \\
&\quad - \sum_{m \neq k} \vartheta_m \boldsymbol{h}_k^{\mathrm{H}}[n-d]\boldsymbol{h}_k[n]\boldsymbol{h}_k^{\mathrm{H}}[n] \\
&\quad \times \boldsymbol{h}_m[n-d]\boldsymbol{h}_m^{\mathrm{H}}[n-d]\boldsymbol{h}_k[n-d] \\
&\quad - \sum_{l \neq k} \vartheta_r \boldsymbol{h}_k^{\mathrm{H}}[n-d]\boldsymbol{h}_r[n-d]\boldsymbol{h}_r^{\mathrm{H}}[n-d] \\
&\quad \times \boldsymbol{h}_k[n]\boldsymbol{h}_k^{\mathrm{H}}[n]\boldsymbol{h}_k[n-d] \\
&\quad + \sum_{r \neq k} \sum_{m \neq k} \vartheta_r \vartheta_m \boldsymbol{h}_k^{\mathrm{H}}[n-d]\boldsymbol{h}_r[n-d]\boldsymbol{h}_r^{\mathrm{H}}[n-d]\boldsymbol{h}_k[n]\boldsymbol{h}_k^{\mathrm{H}}[n] \\
&\quad \times \boldsymbol{h}_m[n-d]\boldsymbol{h}_m^{\mathrm{H}}[n-d]\boldsymbol{h}_k[n-d]. \quad (29)
\end{aligned}$$

Using the lemmas 4 and 5 in [36] and using the temporal correlations across consecutive channel realizations, we can simplify as follows,

$$\begin{aligned}
&\boldsymbol{h}_k^{\mathrm{H}}[n-d]\boldsymbol{h}_k[n]\boldsymbol{h}_k^{\mathrm{H}}[n]\boldsymbol{h}_k[n-d] \\
&= |\rho|^2 \boldsymbol{x}_k^{\mathrm{H}}[n-d]\boldsymbol{R}_k\boldsymbol{x}_k[n-d] \\
&\quad + \left(1 - |\rho|^2\right) \boldsymbol{x}_k^{\mathrm{H}}[n-d]\boldsymbol{R}_k\boldsymbol{w}_k[n]\boldsymbol{w}_k^{\mathrm{H}}[n]\boldsymbol{R}_k\boldsymbol{x}_k[n-d] \\
&= |\rho|^2 \operatorname{tr}^2(\boldsymbol{R}_k) + \left(1 - |\rho|^2\right) \operatorname{tr}\left(R_k^2\right) \\
&\boldsymbol{h}_k^{\mathrm{H}}[n-d]\boldsymbol{h}_k[n]\boldsymbol{h}_k^{\mathrm{H}}[n]\boldsymbol{h}_m[n-d]\boldsymbol{h}_m^{\mathrm{H}}[n-d]\boldsymbol{h}_k[n-d] \\
&= |\rho|^2 \boldsymbol{x}_k^{\mathrm{H}}[n-d]\boldsymbol{R}_k\boldsymbol{x}_k[n-d]\boldsymbol{x}_k^{\mathrm{H}}[n-d]\boldsymbol{R}_m\boldsymbol{R}_k\boldsymbol{x}_k[n-d] \\
&\quad + \left(1 - |\rho|^2\right) \boldsymbol{x}_k^{\mathrm{H}}[n-d]\boldsymbol{R}_k\boldsymbol{w}_k[n]\boldsymbol{w}_k^{\mathrm{H}}[n]\boldsymbol{R}_m\boldsymbol{R}_k\boldsymbol{x}_k[n-d] \\
&= |\rho|^2 \operatorname{tr}(\boldsymbol{R}_k) \operatorname{tr}(\boldsymbol{R}_k\boldsymbol{R}_m) + (1 - |\rho|^2) \operatorname{tr}(\boldsymbol{R}_k\boldsymbol{R}_m\boldsymbol{R}_k)
\end{aligned}$$

Similarly,

$$\begin{aligned}
&\boldsymbol{h}_k^{\mathrm{H}}[n-d]\boldsymbol{h}_r[n-d]\boldsymbol{h}_r^{\mathrm{H}}[n-d]\boldsymbol{h}_k[n]\boldsymbol{h}_k^{\mathrm{H}}[n]\boldsymbol{h}_k[n-d] \\
&\quad = |\rho|^2 \operatorname{tr}(\boldsymbol{R}_k\boldsymbol{R}_r) \operatorname{tr}(\boldsymbol{R}_k) + (1 - |\rho|^2) \operatorname{tr}\left(\boldsymbol{R}_k^2\boldsymbol{R}_r\right)
\end{aligned}$$

Also, $\sum_{r \neq k} \sum_{m \neq k} \vartheta_r \vartheta_m \boldsymbol{h}_k^{\mathrm{H}}[n-d]\boldsymbol{h}_r[n-d]\boldsymbol{h}_r^{\mathrm{H}}[n-d]\boldsymbol{h}_k[n]\boldsymbol{h}_k^{\mathrm{H}}[n] \times \boldsymbol{h}_m[n-d]\boldsymbol{h}_m^{\mathrm{H}}[n-d]\boldsymbol{h}_k[n-d]$ can be split into two cases as $r \neq m$ and $r = m$. When $r \neq m$,

$$\begin{aligned}
&\boldsymbol{h}_k^{\mathrm{H}}[n-d]\boldsymbol{h}_r[n-d]\boldsymbol{h}_r^{\mathrm{H}}[n-d]\boldsymbol{h}_k[n]\boldsymbol{h}_k^{\mathrm{H}}[n]\boldsymbol{h}_m[n-d]\boldsymbol{h}_m^{\mathrm{H}}[n-d] \\
&\quad \times \boldsymbol{h}_k[n-d] \\
&\quad = |\rho|^2 \operatorname{tr}(\boldsymbol{R}_k\boldsymbol{R}_r) \operatorname{tr}(\boldsymbol{R}_k\boldsymbol{R}_m) + (1 - |\rho|^2 \operatorname{tr}(\boldsymbol{R}_k\boldsymbol{R}_m\boldsymbol{R}_r)).
\end{aligned}$$

and when $r = m$,

$$\begin{aligned}
&\boldsymbol{h}_k^{\mathrm{H}}[n-d]\boldsymbol{h}_r[n-d]\boldsymbol{h}_r^{\mathrm{H}}[n-d]\boldsymbol{h}_k[n]\boldsymbol{h}_k \\
&\quad \times^{\mathrm{H}}[n]\boldsymbol{h}_r[n-d]\boldsymbol{h}_r^{\mathrm{H}}[n-d]\boldsymbol{h}_k[n-d] \\
&= |\rho|^2 \operatorname{tr}^2(\boldsymbol{R}_k^{0.5}\boldsymbol{R}_r^{0.5}) \operatorname{tr}(\boldsymbol{R}_r^{0.5}\boldsymbol{R}_k^{0.5}) + (1 - |\rho|^2) \operatorname{tr}^2(\boldsymbol{R}_k^{0.5}\boldsymbol{R}_r^{0.5}).
\end{aligned}$$

Substituting the expressions, we get the numerator term of SINR. Similarly, we can prove the interference term and noise terms. Because of the space constraints, we are omitting the derivation of the same here.

ACKNOWLEDGMENT

The authors would like to thank the British Telecom India Research Centre, for the help and support in making this work possible.

REFERENCES

[1] H. Q. Ngo, A. Ashikhmin, H. Yang, E. G. Larsson, and T. L. Marzetta, "Cell-free massive MIMO versus small cells," *IEEE Trans. Wireless Commun.*, vol. 16, no. 3, pp. 1834–1850, Mar. 2017.
[2] E. Björnson and L. Sanguinetti, "Making cell-free massive MIMO competitive with MMSE processing and centralized implementation," *IEEE Trans. Wireless Commun.*, vol. 19, no. 1, pp. 77–90, Jan. 2020.
[3] E. Björnson and L. Sanguinetti, "Scalable cell-free massive MIMO systems," *IEEE Trans. Commun.*, vol. 68, no. 7, pp. 4247–4261, Jul. 2020.
[4] G. Interdonato, E. Björnson, H. Q. Ngo, P. Frenger, and E. G. Larsson, "Ubiquitous cell-free massive MIMO communications," *EURASIP J. Wireless Commun. Netw.*, vol. 2019, no. 1, pp. 1–13, Dec. 2019.
[5] J. Qiu, K. Xu, X. Xia, Z. Shen, and W. Xie, "Downlink power optimization for cell-free massive MIMO over spatially correlated Rayleigh fading channels," *IEEE Access*, vol. 8, pp. 56214–56227, 2020.
[6] A. Á. Polegre, F. Riera-Palou, G. Femenias, and A. G. Armada, "Channel hardening in cell-free and user-centric massive MIMO networks with spatially correlated Ricean fading," *IEEE Access*, vol. 8, pp. 139827–139845, 2020.
[7] K. T. Truong and R. W. Heath, "Effects of channel aging in massive MIMO systems," *J. Commun. Netw.*, vol. 15, no. 4, pp. 338–351, Aug. 2013.
[8] C. Kong, C. Zhong, A. K. Papazafeiropoulos, M. Matthaiou, and Z. Zhang, "Sum-rate and power scaling of massive MIMO systems with channel aging," *IEEE Trans. Commun.*, vol. 63, no. 12, pp. 4879–4893, Dec. 2015.
[9] S. Biswas and P. Vijayakumar, "AP selection in cell-free massive MIMO system using machine learning algorithm," in *Proc. 6th Int. Conf. Wireless Commun., Signal Process. Netw. (WiSPNET)*, Mar. 2021, pp. 158–161.
[10] M. Alonzo, S. Buzzi, A. Zappone, and C. D'Elia, "Energy-efficient power control in cell-free and user-centric massive MIMO at millimeter wave," *IEEE Trans. Green Commun. Netw.*, vol. 3, no. 3, pp. 651–663, Sep. 2019.
[11] M. Attarifar, A. Abbasfar, and A. Lozano, "Subset MMSE receivers for cell-free networks," *IEEE Trans. Wireless Commun.*, vol. 19, no. 6, pp. 4183–4194, Jun. 2020.
[12] S. Xia, C. Ge, R. Takahashi, Q. Chen, and F. Adachi, "A study on cluster-centric cell-free massive MIMO system," in *Proc. 27th Asia Pacific Conf. Commun. (APCC)*, Oct. 2022, pp. 247–252.
[13] H. T. Dao and S. Kim, "Effective channel gain-based access point selection in cell-free massive MIMO systems," *IEEE Access*, vol. 8, pp. 108127–108132, 2020.
[14] S. Buzzi and C. D'Andrea, "Cell-free massive MIMO: User-centric approach," *IEEE Wireless Commun. Lett.*, vol. 6, no. 6, pp. 706–709, Dec. 2017.
[15] S. Buzzi, C. D'Andrea, A. Zappone, and C. D'Elia, "User-centric 5G cellular networks: Resource allocation and comparison with the cell-free massive MIMO approach," *IEEE Trans. Wireless Commun.*, vol. 19, no. 2, pp. 1250–1264, Feb. 2020.
[16] F. Riera-Palou, G. Femenias, A. G. Armada, and A. Pérez-Neira, "Clustered cell-free massive MIMO," in *Proc. IEEE Globecom Workshops (GC Wkshps)*, Dec. 2018, pp. 1–6.
[17] O. Zhou, J. Wang, and F. Liu, "Average downlink rate analysis for clustered cell-free networks with access point selection," in *Proc. IEEE Int. Symp. Inf. Theory (ISIT)*, Jun. 2022, pp. 742–747.
[18] R. Wang, M. Shen, Y. He, and X. Liu, "Performance of cell-free massive MIMO with joint user clustering and access point selection," *IEEE Access*, vol. 9, pp. 40860–40870, 2021.

[19] Q. N. Le, V. Nguyen, O. A. Dobre, N. Nguyen, R. Zhao, and S. Chatzinotas, "Learning-assisted user clustering in cell-free massive MIMO-NOMA networks," *IEEE Trans. Veh. Technol.*, vol. 70, no. 12, pp. 12872–12887, Dec. 2021.
[20] A. K. Papazafeiropoulos and T. Ratnarajah, "Uplink performance of massive MIMO subject to delayed CSIT and anticipated channel prediction," in *Proc. IEEE Int. Conf. Acoust., Speech Signal Process. (ICASSP)*, May 2014, pp. 3162–3165.
[21] A. K. Papazafeiropoulos, "Downlink performance of massive MIMO under general channel aging conditions," in *Proc. IEEE Global Commun. Conf. (GLOBECOM)*, Dec. 2015, pp. 1–6.
[22] A. K. Papazafeiropoulos, "Impact of general channel aging conditions on the downlink performance of massive MIMO," *IEEE Trans. Veh. Technol.*, vol. 66, no. 2, pp. 1428–1442, Feb. 2017.
[23] R. Chopra, C. R. Murthy, H. A. Suraweera, and E. G. Larsson, "Performance analysis of FDD massive MIMO systems under channel aging," *IEEE Trans. Wireless Commun.*, vol. 17, no. 2, pp. 1094–1108, Feb. 2018.
[24] W. Peng, W. Li, W. Wang, X. Wei, and T. Jiang, "Downlink channel prediction for time-varying FDD massive MIMO systems," *IEEE J. Sel. Topics Signal Process.*, vol. 13, no. 5, pp. 1090–1102, Sep. 2019.
[25] M. M. Taygur and T. F. Eibert, "Analyzing the channel aging effects on massive MIMO downlink by ray-tracing," in *Proc. IEEE 29th Annu. Int. Symp. Pers., Indoor Mobile Radio Commun. (PIMRC)*, Sep. 2018, pp. 1–5.
[26] W. Jiang and H. D. Schotten, "Impact of channel aging on zero-forcing precoding in cell-free massive MIMO systems," *IEEE Commun. Lett.*, vol. 25, no. 9, pp. 3114–3118, Sep. 2021.
[27] J. Zheng, J. Zhang, E. Björnson, and B. Ai, "Impact of channel aging on cell-free massive MIMO over spatially correlated channels," *IEEE Trans. Wireless Commun.*, vol. 20, no. 10, pp. 6451–6466, Oct. 2021.
[28] R. Chopra, C. R. Murthy, and A. K. Papazafeiropoulos, "Uplink performance analysis of cell-free massive MIMO systems under channel aging," *IEEE Commun. Lett.*, vol. 25, no. 7, pp. 2206–2210, Jul. 2021.
[29] E. Björnson, J. Hoydis, and L. Sanguinetti, "Massive MIMO networks: Spectral, energy, and hardware efficiency," *Found. Trends Signal Process.*, vol. 11, nos. 3–4, pp. 154–655, 2017.
[30] *Further Advancements for E-UTRA Physical Layer Aspects (Release 9)*, Standard ETSI TR 136 913, 3rd Generation Partnership Project (3GPP), 3GPP, Tech. Rep., Mar. 2017. [Online]. Available: https://www.3gpp.org/ftp//Specs/archive/36_series/36.814/36814-f40.zip
[31] R. Couillet and M. Debbah, *Random Matrix Methods for Wireless Commun*. Cambridge, U.K.: Cambridge Univ. Press, 2011.
[32] A. K. Papazafeiropoulos, H. Q. Ngo, M. Matthaiou, and T. Ratnarajah, "Uplink performance of conventional and massive MIMO cellular systems with delayed CSIT," in *Proc. IEEE 25th Annu. Int. Symp. Pers., Indoor, Mobile Radio Commun. (PIMRC)*, Sep. 2014, pp. 601–606.
[33] A. Khalili, A. Ashikhmin, and H. Yang, "Cell-free massive MIMO with low-complexity hybrid beamforming," 2021, *arXiv:2111.07463*.
[34] G. H. Golub and C. F. Van Loan, *Matrix Computer*. Baltimore, MD, USA: JHU Press, 2013.
[35] J. W. Silverstein and Z. D. Bai, "On the empirical distribution of eigenvalues of a class of large dimensional random matrices," *J. Multivariate Anal.*, vol. 54, no. 2, pp. 175–192, Aug. 1995.
[36] S. Wagner, R. Couillet, M. Debbah, and D. T. M. Slock, "Large system analysis of linear precoding in correlated MISO broadcast channels under limited feedback," *IEEE Trans. Inf. Theory*, vol. 58, no. 7, pp. 4509–4537, Jul. 2012.

MARIA FRANCIS (Student Member, IEEE) received the B.Tech. degree in electronics and communication from the Cochin University of Science and Technology and the M.Tech. degree in communication systems from the Thangal Kunju Musaliar College, Kollam, Kerala, India. She is currently pursuing the Ph.D. degree in electrical communication engineering with the Indian Institute of Science, Bengaluru. Her research interests include wireless communications, 5G, and emerging technologies in wireless communication.

FARHAD MEHRAN (Senior Member, IEEE) received the M.Eng. degree in electronic and communications engineering from the University of Birmingham, U.K., in 2009, and the Ph.D. degree from the Institute for Communication Systems, Home of 5G & 6G Innovation Centre, University of Surrey, Guildford, U.K., in 2020. Throughout his career, he worked in close collaboration with leading telecom research institutions with the University of California at Irvine, the University of Surrey, and the University of Southampton, and authored more than ten IEEE paper publications. In 2016, he joined the Wireless Research Team, BT Research and Innovation, U.K., where he was working on physical and systems aspects of wireless communications. He has extensive experience in project management and research and development of transmission technologies and architectures for 4G LTE/LTE-A and 5G NR systems and holds seven granted inventions in these areas. He received a Chartered Engineer status of the IET, in April 2022.

K. V. S. HARI received the Ph.D. degree in systems science from UC San Diego.

He has been a Visiting Faculty with Stanford University and an Affiliate Professor with the KTH Royal Institute of Technology, Stockholm. He is currently a Professor with the Department of ECE, Indian Institute of Science (IISc), Bengaluru. He has been part of the Indo-U.K. Advanced Technology Centre (IU-ATC). He also leads the British Telecom India Research Centre (BTIRC), IISc. He is the coauthor of the IEEE 802.16 standard on wireless channel models and has conducted drone-ground wireless channel modeling experiments. His research interests include signal processing and deep learning with applications to 5G wireless communications, indoor positioning, dual-function radar and communication systems, autonomous navigation, neuroscience, and affordable MRI systems.

Dr. Hari is a fellow of the Indian National Academy of Engineering and the Indian National Science Academy. He was an Editor of *Journal on Advances in Signal Processing* (EURASIP). He is also the Editor-in-Chief (Electrical Sciences) of *Sadhana* and the *Journal of the Indian Academy of Sciences* (Springer). He was on the Board of Governors of the IEEE Signal Processing Society as VP-Membership. He served as the Chair for the Standardization Committee, Telecom Standards Development Society, India. More details at http://ece.iisc.ac.in/hari/